CORRELATION-MODEL OF ROTOR-EFFECTIVE WIND SHEARS AND WIND SPEED FOR LIDAR-BASED INDIVIDUAL PITCH CONTROL

Florian Haizmann, David Schlipf, Po Wen Cheng

Stuttgart Wind Energy (SWE), University of Stuttgart, Germany, haizmann@ifb.uni-stuttgart.de

Summary

In this work the spectra based model of the correlation between lidar systems and wind turbines is extended from rotor-effective wind speed only, to rotor-effective wind speed and linear horizontal and vertical shear components. This is achieved by the incorporation of a model based wind field reconstruction method solving a set of linear equations with the least-squares method. The model allows to optimize a lidar system's measurement configuration for a specific wind turbine a-priori by means of direct and fast spectra calculations. Furthermore, it allows to assess the filter parameters to be expected and needed for the application of lidar-assisted control. By extending the model to rotor-effective linear shears, the results can be used for lidar-assisted individual pitch control.

1. Introduction

The application of lidar systems for preview-based control concepts of wind turbines has been widely proposed during the last years in wind energy research. At the same time wind turbine manufacturers are increasingly interested in this technology and there is a growing range of lidar systems available on the market. However, the commercially available systems are not yet very flexible regarding their measurement configuration, like for example the number of measurement points or their spacial distribution over the rotor disc.

SWE is using its highly flexible, scanning lidar system to study the influence of different lidar measurement configurations on different wind turbines and for different applications of lidars. In the course of this research a spectra based model of the correlation between rotor-effective wind speed – measured by a lidar and experienced by a wind turbine – has been developed [1]. This model makes use of a direct calculation of the lidar and rotor cross- and auto-spectra of the rotor-effective wind speed, which are much faster than time domain simulations. Therefore, the model can help lidar system users to asses and increase the suitability of a lidar for their application a-priori. The model has been successfully used to optimize the measurement configurations of different lidar systems for field-testing of lidar-assisted collective pitch feed-forward controllers [2, 3] and shows good agreement with field-test data. In [4], the approach has been extended to blade effective wind speeds.

The presented work further develops the correlation-model by extending it from calculating the spectrum of the rotor-effective wind speed only to the calculation of the spectrum of the rotor-effective wind speed as well as the spectra of the linear rotor-effective horizontal and vertical wind shear components. Therefore, it becomes applicable to lidar-assisted individual pitch feed-forward control.

This paper is organized as follows: Section 2 summarizes the basic principle of the correlation-model and elaborates its extension. Section 3 presents the validation of the extension for different effects. In Section 4 an exemplary optimization of a lidar measurement trajectory is shown and Section 5 concludes the paper.

2. The Correlation-Model

The basic idea of the spectra-based correlation-model is to calculate the correlation between the rotor-effective wind speed measured by a lidar system and the one experienced by a wind turbine directly from the spectral properties of a wind field as shown in Figure 1. The equations for the lidar measurement and the wind reconstruction are transferred by Fourier transformation into the frequency domain to avoid time-consuming simulations in the time-domain and to provide an analytic form rather than an estimation of the correlation.

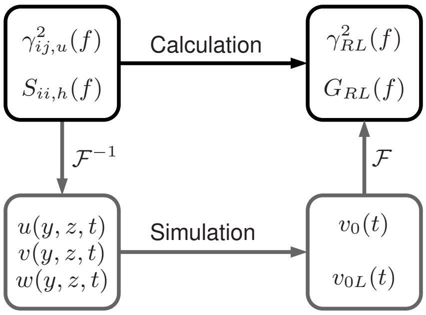

Figure 1: Basic idea of the correlation model. Equations are transferred from time-domain (gray) to frequency-domain (black).

2.1. Mathematical Background

The correlation between the rotor-effective wind speed measured by the lidar and experienced by the wind turbine's rotor is expressed by the magnitude squared coherence γ^2_{RL}, defined as

$$\gamma^2_{RL} = \frac{|S_{RL}|^2}{S_{RR}S_{LL}}, \quad (1)$$

where S_{RL}, S_{RR}, and S_{LL} are the cross-spectrum between both signals and the auto-spectrum of the signal from the turbine and the lidar, respectively. The auto-spectra of the rotor-effective wind speed v_0 and its lidar estimate v_{0L} and the cross-spectrum between them is defined – omitting all scaling constants and mean operators – by

$$\begin{aligned} S_{RR} &= \mathcal{F}\{v_0\}\mathcal{F}^*\{v_0\} \\ S_{RL} &= \mathcal{F}\{v_0\}\mathcal{F}^*\{v_{0L}\} \\ S_{LL} &= \mathcal{F}\{v_{0L}\}\mathcal{F}^*\{v_{0L}\}, \end{aligned} \quad (2)$$

where $\mathcal{F}\{\}$ and $\mathcal{F}^*\{\}$ are the Fourier transform and its complex conjugate, respectively [5]. Using these definitions, the correlation-model calculates the spectra semi-analytically by processing a summation of numerous spectra – all originating from the IEC Kaimal spectral wind model – including amongst others the following effects:

- Spacial averaging of the lidar measurement.
- Discrete sampling of the single lidar measurements.
- Reconstructing the rotor-effective wind speed by averaging over all measured longitudinal wind components in a single focus distance.
- Averaging the rotor-effective wind speed over several focus distances.

2.2. Extension to Wind Shears

In order to extend the correlation-model to wind shears the underlying wind model is changed. Assuming, that there is no tilted inflow and no misalignment present (no lateral $v_{i,\mathcal{W}}$ and no vertical wind component $w_{i,\mathcal{W}}$) the longitudinal wind component can be expressed as

$$u_{i,\mathcal{W}} = v_0 + \delta_H y_{i,\mathcal{W}} + \delta_V z_{i,\mathcal{W}}, \tag{3}$$

where v_0 is the rotor-effective wind speed and δ_H and δ_V are the linear rotor-effective horizontal and vertical shears. $[x_{i,\mathcal{W}}\ y_{i,\mathcal{W}}\ z_{i,\mathcal{W}}]^T$ are the coordinates of the i-th lidar focus point in the wind coordinate system ($\mathcal{W}$) [6]. Combining the wind model (3) with the lidar measurement equation

$$v_{los,i} = \frac{x_{i,\mathcal{W}}}{f_{i,\mathcal{W}}} u_{i,\mathcal{W}} + \frac{y_{i,\mathcal{W}}}{f_{i,\mathcal{W}}} v_{i,\mathcal{W}} + \frac{z_{i,\mathcal{W}}}{f_{i,\mathcal{W}}} w_{i,\mathcal{W}}, \tag{4}$$

where $v_{los,i}$ is the Line-Of-Sight lidar measurement at focus point i, the following linear system of equations for the three unknown wind characteristics is obtained:

$$\begin{bmatrix} v_{los,1} \\ \vdots \\ v_{los,n} \end{bmatrix} = \underbrace{\begin{bmatrix} \frac{x_{1,\mathcal{W}}}{f_{1,\mathcal{W}}} & \frac{x_{1,\mathcal{W}}}{f_{1,\mathcal{W}}} y_{1,\mathcal{W}} & \frac{x_{1,\mathcal{W}}}{f_{1,\mathcal{W}}} z_{1,\mathcal{W}} \\ \vdots & \vdots & \vdots \\ \frac{x_{n,\mathcal{W}}}{f_{n,\mathcal{W}}} & \frac{x_{n,\mathcal{W}}}{f_{n,\mathcal{W}}} y_{n,\mathcal{W}} & \frac{x_{n,\mathcal{W}}}{f_{n,\mathcal{W}}} z_{n,\mathcal{W}} \end{bmatrix}}_{A} \begin{bmatrix} v_0 \\ \delta_H \\ \delta_V \end{bmatrix}. \tag{5}$$

For $n = 3$ the solution can be found by calculating the inverse of A:

$$\begin{bmatrix} v_0 \\ \delta_H \\ \delta_V \end{bmatrix} = A^{-1} \begin{bmatrix} v_{los,1} \\ v_{los,2} \\ v_{los,3} \end{bmatrix}. \tag{6}$$

In the case of $n > 3$ focus points the solution can be found by using the least-squares method and calculating the Moore–Penrose pseudoinverse of A.

Besides the incorporation of the calculation of the (pseudo-)inverse of A, the correlation-model needs no further structural changes to its algorithms since the new wind reconstruction consists of linear equations. Therefore, the Fourier transform of the wind characteristics can be expressed as before by a sum of wind spectra due to the linearity of the Fourier transformation.

3. Validation of the Extension

The new correlation-model is validated comparing the lidar spectra of v_0, δ_H and δ_V respectively from a time-domain simulation and from the model.

In the following, the validation is shown for different effects included in the correlation-model step-by-step starting with a perfect measurement. For all examined cases, the focus points are acquired simultaneously in the simulation as well as by the model. Furthermore, the model does not include any wind evolution, since the longitudinal decay is also not considered in the time-domain simulations. However, it can be included similar to [1], if used along with real measurements.

3.1. Perfect Lidar Measurement

As explained in Section 2.2, at least three focus points are needed to be able to find a solution for the three wind characteristics. Therefore, the first and simplest validation uses three focus points and assumes a perfect measurement in the focus points without any volume averaging.

Figure 2(a) shows the lidar spectra of the three wind characteristics. Apart from inaccuracies resulting from the spectra estimation process from the non-endless simulation data, the spectra show perfect agreement for all three characteristics.

3.2. Spatial Averaging

A real lidar system averages the wind speeds along the laser beam according to a system specific weighting function. In simulation as well as by the correlation-model, this is considered by evaluating such a weighting function at discrete distances around the focus point along the laser beam. Here, a typical range weighting function of a pulsed lidar system is used and evaluated and discretized at three points.

Figure 2(b) shows again a good agreement of the model with the simulation for all three wind characteristics.

3.3. More than Three Measurement Points

As described in Section 2.2 the model needs to calculate the solution for v_0, δ_H and δ_V by means of the Moore–Penrose pseudoinverse of A for more than three measurement points. This is validated with a trajectory containing four focus points. Again, perfect measurement is assumed for the validation.

3.4. Multiple Focus Distances

The last validation aims on the combination of several focus distances which can be acquired by a pulsed lidar system at the same time. The three wind characteristics are calculated individually for each focus distance and afterwards shifted according to Taylor's Frozen Turbulence Hypothesis before they are averaged. For this purpose a trajectory with three focus points, in two focus distances and perfect measurement is taken.

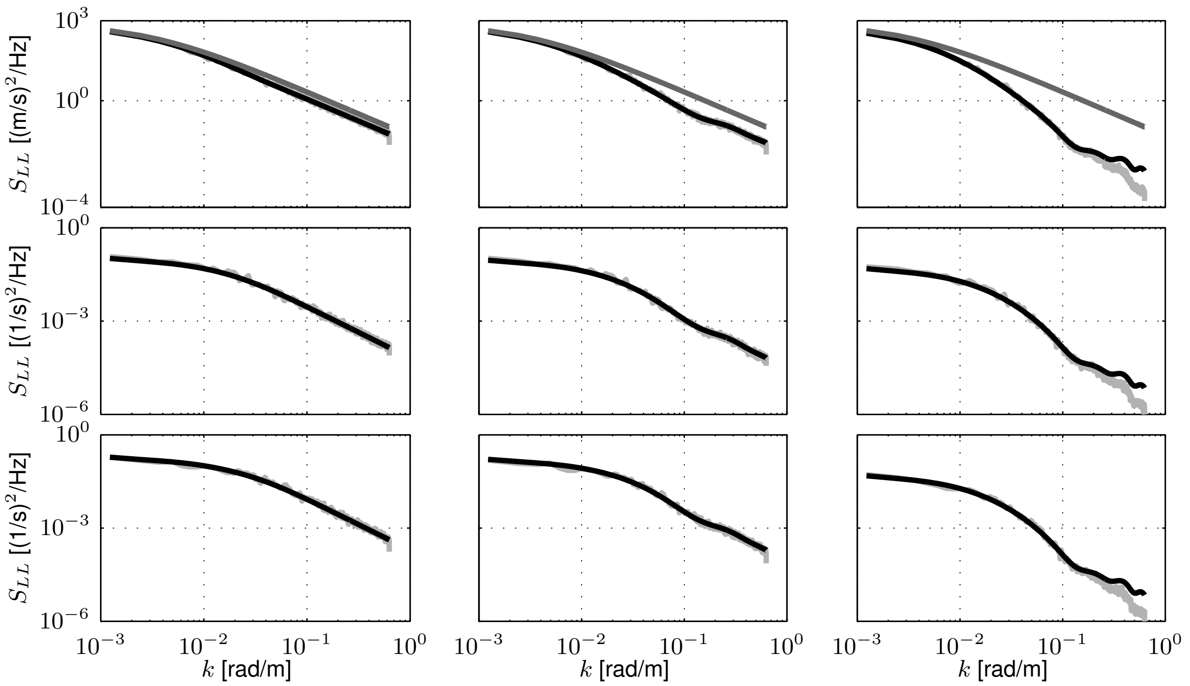

(a) Perfect three beam measurement.

(b) Three beam measurement with spacial averaging.

(c) Four beam measurement with spacial averaging and five focus distances.

Figure 2: Lidar spectra for v_0 (top), δ_H (middle) and δ_V (bottom) from model (black), from simulation (light gray) and with wind spectrum (dark gray).

3.5. Combination of Effects

Finally, the last case shows the combination of all individually validated effects. Therefore, a lidar trajectory with four focus points, five focus distances, and a typical range weighting function of a pulsed lidar system is chosen.
The combined performance of the correlation-model is shown in Figure 2(c). Up to about $k = 0.15\ \mathrm{rad/m}$ the model and the simulation agree perfectly. Beyond this wavenumber, the model reflects the correct shape of the three spectra, but the simulated spectra are reduced too strongly due to limitations of the estimation process of the spectra from time series data.

4. Exemplary Trajectory Optimization

One of the main applications of the correlation-model is the optimization of a lidar measurement configuration for a specific turbine. In this section the results of an exemplary optimization of the trajectory from Section 3.5 is shown. The fixed parameters are as follows: The trajectory consists of four focus points, which are pointing exactly up, down, to the left and to the right of the rotor disk, and it has five focus distances, of which the furthest one is located at $1.5D$. The wind turbine used is the NREL $5\ \mathrm{MW}$ reference turbine with a rotor diameter of $D = 126\ \mathrm{m}$.
The parameters for the optimization are:

- The position of the first focus distance $x_{1,\mathcal{L}}$ (normalized by D) in the lidar coordinate system ($\mathcal{L}$). The remaining focus distances are positioned equally between the first and the fifth.
- The width of the scan, represented by the absolute distance of the four points in lateral and vertical direction from the centre at the first focus distance $yz_{1,\mathcal{L}}$ (normalized by D).

As the measure of optimality the coherence bandwidth is used, which is defined as the wavenumber $k_{0.5}$, where the magnitude squared coherence γ^2_{RL} reaches 0.5. Figure 3 shows $k_{0.5}$ for the three wind characteristics v_0, δ_H and δ_V, respectively in dependence of the two optimization parameters. While δ_H and δ_V show very similar results for $k_{0.5}$, they differ strongly from the result for v_0. The optimal trajectory for v_0 has its first focus distance rather close ($x_{1,\mathcal{L}} = 0.5D$) and uses a small opening ($yz_{1,\mathcal{L}} = 0.15D$). Whereas the optimal trajectory for δ_H and δ_V has its first focus distance further away ($x_{1,\mathcal{L}} = 0.7D$) and uses a bigger opening ($yz_{1,\mathcal{L}} = 0.25D$). This means that for reconstructing the linear shear components it is better to scan the wind field in front of a wind turbine over a bigger area of the rotor disk, which is contrary to the optimal scan for the wind speed. In order to reconstruct both at the same time, it is necessary to find a compromise between the two optimal configurations.

In general, the correlation of the rotor-effective linear wind shear components has a worse coherence compared to the wind speed as shown in Figure 4. This reduced coherence requires a different filtering of the shear components compared to the wind speed before using those as inputs to a feed-forward individual pitch controller.

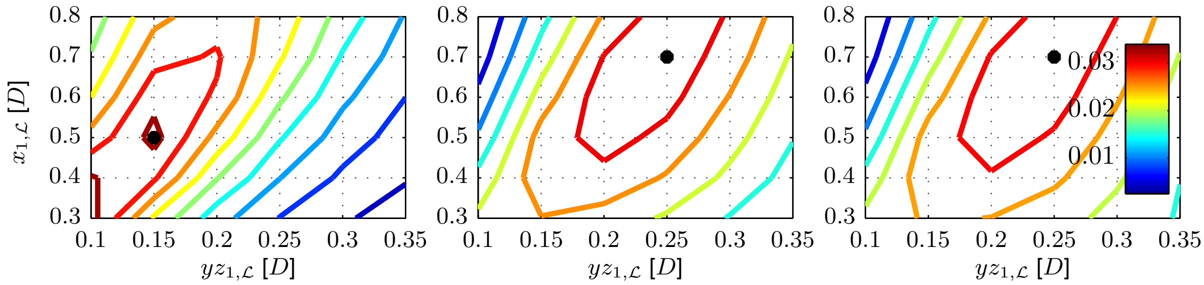

Figure 3: Coherence bandwidth $k_{0.5}$ for v_0 (left), δ_H (middle) and δ_V (right) with corresponding optima (•).

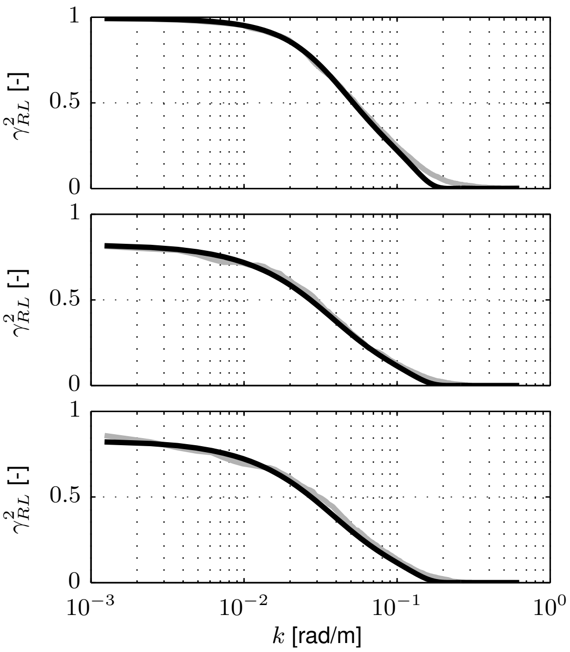

Figure 4: Coherence between the lidar estimate and the rotor-effective v_0 (top), δ_H (middle) and δ_V (bottom) from the wind-field based on model (black) and from simulation (light gray) using the optimal trajectory for v_0.

5. Conclusion and Outlook

In this work, the spectra based model for the correlation of the rotor-effective wind speed measured by a lidar and experienced by a wind turbine is extended to the linear horizontal and vertical shears δ_H and δ_V. The extension is done by a change of the underlying wind model and validated stepwise with regard to different effects. The validation confirms the correct implementation of the new wind model and the new reconstruction method.

In a second step, the new model is used to perform an exemplary trajectory optimization of a simple four beam configuration. As a result of this it is shown that the optimal trajectory configuration differs significantly for the rotor-effective wind speed and the two linear rotor-effective shears, respectively. This means that a compromise needs to be found for reconstructing all three wind characteristics at the same time. Furthermore, it is found out that the wind shears have generally a lower coherence for such a trajectory, which requires different filtering for lidar-assisted control applications.

As an outlook to further utilization and developments of the SWE correlation-model it can be mentioned that a good criteria for finding a compromise trajectory needs to be developed. Furthermore, more complex trajectories with more focus points and different layouts need to be examined and the extension needs to be validated for further effects like e.g. consecutive scanning.

Acknowledgment

Part of this research is funded by the German Federal Ministry for Economic Affairs and Energy (BMWi) in the framework of the German joint research project "Triple I Blade Control" by Senvion SE in cooperation with Technische Universität Darmstadt and SWE.

References

[1] Schlipf, D., Mann, J., and Cheng, P. W., "Model of the Correlation between Lidar Systems and Wind Turbines for Lidar Assisted Control," *Journal of Atmospheric and Oceanic Technology*, Vol. 30, No. 10, 2013, pp. 2233–2240.

[2] Haizmann, F., Schlipf, D., Raach, S., Scholbrock, A., Wright, A., Slinger, C., Medley, J., Harris, M., Bossanyi, E., and Cheng, P. W., "Optimization of a Feed-Forward Controller Using a CW-lidar System on the CART3," Paper accepted for presentation at American Control Conference, 2015.

[3] Schlipf, D., Haizmann, F., Cosack, N., Siebers, T., and Cheng, P. W., "Detection of Wind Evolution and Lidar Trajectory Optimization for Lidar-AssistedWind Turbine Control," Paper submitted to Meteorologische Zeitschrift, in editing, 2015.

[4] Simley, E. and Pao, L., "Correlation between Rotating LIDAR Measurements and Blade Effective Wind Speed," *Proc. AIAA Aerospace Sciences Meeting*, Grapevine,TX, USA, 2013.

[5] Bendat, J. S. and Piersol, A. G., *Random data; analysis and measurement procedures*, John Wiley & Sons, New York, USA, 1971.

[6] Schlipf, D., Kapp, S., Anger, J., Bischoff, O., Hofsäß, M., Rettenmeier, A., Smolka, U., and Kühn, M., "Prospects of Optimization of Energy Production by LiDAR Assisted Control of Wind Turbines," *Proceedings of the EWEA Annual event*, Brussels, Belgium, 2011.